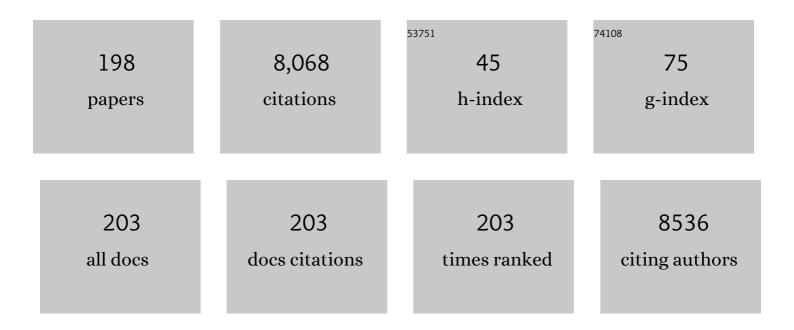
List of Publications by Year in descending order

Source: https://exaly.com/author-pdf/832415/publications.pdf Version: 2024-02-01



#	Article	lF	CITATIONS
1	Enhancing the adsorption function of F- by iron and zirconium doped zeolite: Characterization and parameter optimization. Environmental Engineering Research, 2023, 28, 220010-0.	1.5	2
2	The Current Status of Hazardous Waste Management in China: Identification, Distribution, and Treatment. Environmental Engineering Science, 2022, 39, 81-97.	0.8	12
3	High-hydrophilic and antifouling reverse osmosis membrane prepared based an unconventional radiation method for pharmaceutical plant effluent treatment. Separation and Purification Technology, 2022, 280, 119838.	3.9	18
4	Nickel dual-atom catalysts for the selective electrocatalytic debromination of tribromoacetic acid as a green chemistry process. Chemical Engineering Journal, 2022, 427, 131719.	6.6	24
5	Activated carbon modified with nano manganese dioxide triggered electron transport pathway changes for boosted anaerobic treatment of dyeing wastewater. Environmental Research, 2022, 203, 111944.	3.7	20
6	Activation of sodium persulfate by TiO2@MIL-101(Fe): Boosting the Fenton-like process by interfacial charge transfer. Chemosphere, 2022, 288, 132666.	4.2	15
7	A novel membrane-promoted crystallization process integrating water recovery and salt production for brine management. Chemical Engineering Journal, 2022, 430, 133022.	6.6	8
8	Iron-based biochar derived from waste-activated sludge enhances anaerobic digestion of synthetic salty organic wastewater for methane production. Bioresource Technology, 2022, 345, 126465.	4.8	33
9	Honeycomb-like holey Co3O4 membrane triggered peroxymonosulfate activation for rapid degradation of organic contaminants. Science of the Total Environment, 2022, 814, 152698.	3.9	36
10	Electro-oxidation of Ni (II)-citrate complexes at BDD electrode and simultaneous recovery of metallic nickel by electrodeposition. Journal of Environmental Sciences, 2022, 116, 103-113.	3.2	24
11	Batch sorption and fixed-bed elution for Pd recovery using stable amine-functionalized melamine sponge. Journal of Cleaner Production, 2022, 337, 130475.	4.6	9
12	Zero valent boron activated ozonation for ultra-fast degradation of organic pollutants: Atomic orbital matching, oxygen spillover and intra-electron transfer. Chemical Engineering Journal, 2022, 434, 134674.	6.6	13
13	Isolation of Anaerobic Bromate-Reducing Bacteria Using Different Carbon Sources and Transcriptomic Insights From Klebsiella variicola Glu3. Frontiers in Microbiology, 2022, 13, 851844.	1.5	2
14	Enhanced bacterial inactivation by activated carbon modified with nano-sized silver oxides: Performance and mechanism. Journal of Environmental Management, 2022, 311, 114884.	3.8	2
15	Copper single-atom catalyst as a high-performance electrocatalyst for nitrate-ammonium conversion. Journal of Hazardous Materials, 2022, 434, 128892.	6.5	34
16	Separation of Fe from wastewater and its use for NOx reduction; a sustainable approach for environmental remediation. Chemosphere, 2022, 303, 135103.	4.2	11
17	Angstrom-confined catalytic water purification within Co-TiOx laminar membrane nanochannels. Nature Communications, 2022, 13, .	5.8	97
18	Utilization of electrochemical treatment and surface reconstruction to achieve long lasting catalyst for NOx removal. Journal of Hazardous Materials, 2021, 401, 123440.	6.5	21

#	Article	IF	CITATIONS
19	Application of central composite design to reveal resin deterioration during the removal of hexavalent chromium from wastewater. Environmental Technology (United Kingdom), 2021, 42, 298-305.	1.2	1
20	Recovery phosphate and ammonium from aqueous solution by the process of electrochemically decomposing dolomite. Chemosphere, 2021, 262, 128357.	4.2	8
21	Sea urchin-like FeOOH functionalized electrochemical CNT filter for one-step arsenite decontamination. Journal of Hazardous Materials, 2021, 407, 124384.	6.5	26
22	Occurrence and removal of bisphenol analogues in wastewater treatment plants and activated sludge bioreactor. Science of the Total Environment, 2021, 758, 143606.	3.9	42
23	Noble metal-free NiCo2S4/CN sheet-on-sheet heterostructure for highly efficient visible-light-driven photocatalytic hydrogen evolution. Journal of Alloys and Compounds, 2021, 853, 157284.	2.8	26
24	Inductive effect as a universal concept to design efficient catalysts for CO ₂ electrochemical reduction: electronegativity difference makes a difference. Journal of Materials Chemistry A, 2021, 9, 4626-4647.	5.2	12
25	Photocatalyst- and additive-free decarboxylative alkylation of <i>N</i> -aryl tetrahydroisoquinolines induced by visible light. Organic Chemistry Frontiers, 2021, 8, 2473-2479.	2.3	23
26	Enhancing the adsorption function of biochar by mechanochemical graphitization for organic pollutant removal. Frontiers of Environmental Science and Engineering, 2021, 15, 1.	3.3	23
27	NiCo-LDH nanosheets strongly coupled with GO-CNTs as a hybrid electrocatalyst for oxygen evolution reaction. Nano Research, 2021, 14, 4783-4788.	5.8	52
28	Phosphate recovery from aqueous solution via struvite crystallization based on electrochemical-decomposition of nature magnesite. Journal of Cleaner Production, 2021, 292, 126039.	4.6	31
29	Broadband Structured Light Multiplexing With Dielectric Meta-Optics. Journal of Lightwave Technology, 2021, 39, 2830-2836.	2.7	7
30	Separation, anti-fouling, and chlorine resistance of the polyamide reverse osmosis membrane: From mechanisms to mitigation strategies. Water Research, 2021, 195, 116976.	5.3	90
31	Recent advances in hybrid wet scrubbing techniques for NOx and SO2 removal: State of the art and future research. Chemosphere, 2021, 273, 129695.	4.2	45
32	Core-shell ZVI@carbon composites reduce phosphate inhibition of ZVI dissolution and enhance methane production in an anaerobic sewage treatment. Water Research, 2021, 199, 117197.	5.3	21
33	Species and formation characteristics of halogenated DBPs in chloramination of tannic acid after biodegradation. Science of the Total Environment, 2021, 781, 146690.	3.9	8
34	Recent innovations for scaling up microbial fuel cell systems: Significance of physicochemical factors for electrodes and membranes materials. Journal of the Taiwan Institute of Chemical Engineers, 2021, 129, 207-226.	2.7	39
35	Targeted degradation of refractory organic compounds in wastewaters based on molecular imprinting catalysts. Water Research, 2021, 203, 117541.	5.3	36
36	Thermally activated epoxy-functionalized carbon as an electrocatalyst for efficient NOx reduction. Carbon, 2021, 182, 516-524.	5.4	16

#	Article	IF	CITATIONS
37	Phylogenetically divergent bacteria consortium from neutral activated sludge showed heightened potential on bioleaching spent lithium-ion batteries. Ecotoxicology and Environmental Safety, 2021, 223, 112592.	2.9	11
38	Photocatalyst and additive-free visible light induced trifluoromethylation–arylation of <i>N</i> -arylacrylamides with Umemoto's reagent. Chemical Communications, 2021, 57, 1030-1033.	2.2	27
39	Co-precipitation with CaCO3 to remove heavy metals and significantly reduce the moisture content of filter residue. Chemosphere, 2020, 239, 124660.	4.2	34
40	Biological removal of pharmaceuticals by Navicula sp. and biotransformation of bezafibrate. Chemosphere, 2020, 240, 124949.	4.2	35
41	Titania–Montmorillonite for the Photocatalytic Removal of Contaminants from Water: Adsorb & Shuttle Process. Environmental Chemistry for A Sustainable World, 2020, , 291-319.	0.3	13
42	Electrochemical oxidation of perfluorooctane sulfonate (PFOS) substitute by modified boron doped diamond (BDD) anodes. Chemical Engineering Journal, 2020, 379, 122280.	6.6	82
43	Peroxymonosulfate enhanced photoelectrocatalytic degradation of ofloxacin using an easily coated cathode. Separation and Purification Technology, 2020, 236, 116301.	3.9	41
44	Nitrogen-doped porous carbon derived from foam polystyrene as an anode material for lithium-ion batteries. Applied Surface Science, 2020, 504, 144398.	3.1	36
45	Developing an equivalent toxicity area approach to comparing toxicity of urban road deposited sediments. Environmental Pollution, 2020, 257, 113588.	3.7	6
46	Algal toxicity, accumulation and metabolic pathways of galaxolide. Journal of Hazardous Materials, 2020, 384, 121360.	6.5	20
47	Selenium(VI) and copper(II) adsorption using polyethyleneimine-based resins: Effect of glutaraldehyde crosslinking and storage condition. Journal of Hazardous Materials, 2020, 386, 121637.	6.5	67
48	Enhanced photocatalytic hydrogen evolution under visible light irradiation by p-type MoS2/n-type Ni2P doped g-C3N4. Applied Surface Science, 2020, 504, 144448.	3.1	42
49	Photocatalyst- and transition-metal-free α-allylation of <i>N</i> -aryl tetrahydroisoquinolines mediated by visible light. Green Chemistry, 2020, 22, 646-650.	4.6	35
50	Characterizing community dynamics and exploring bacterial assemblages in two activated sludge systems. Applied Microbiology and Biotechnology, 2020, 104, 1795-1808.	1.7	11
51	Facile one-pot synthesis of mesoporous g-C ₃ N ₄ nanosheets with simultaneous iodine doping and N-vacancies for efficient visible-light-driven H ₂ evolution performance. Catalysis Science and Technology, 2020, 10, 549-559.	2.1	39
52	NiMn compound nanosheets for electrocatalytic water oxidation: effects of atomic structures and oxidation states. Nanoscale, 2020, 12, 2472-2478.	2.8	17
53	Ultra-rapid detoxification of Sb(III) using a flow-through electro-fenton system. Chemosphere, 2020, 245, 125604.	4.2	21
54	Comparative cytotoxicity of halogenated aromatic DBPs and implications of the corresponding developed QSAR model to toxicity mechanisms of those DBPs: Binding interactions between aromatic DBPs and catalase play an important role. Water Research, 2020, 170, 115283.	5.3	94

#	Article	IF	CITATIONS
55	Highly efficient degradation of 2,2′,4,4′-tetrabromodiphenyl ether through combining surfactant-assisted Zn0 reduction with subsequent Fenton oxidation. Journal of Hazardous Materials, 2020, 385, 121551.	6.5	8
56	One-step phosphite removal by an electroactive CNT filter functionalized with TiO2/CeOx nanocomposites. Science of the Total Environment, 2020, 710, 135514.	3.9	17
57	Investigating toxicity of urban road deposited sediments using Chinese hamster ovary cells and Chlorella Pyrenoidosa. Chemosphere, 2020, 245, 125634.	4.2	8
58	Convenient one-step fabrication and morphology evolution of thin-shelled honeycomb-like structured g-C3N4 to significantly enhance photocatalytic hydrogen evolution. Applied Surface Science, 2020, 506, 145004.	3.1	22
59	One-step Sb(III) decontamination using a bifunctional photoelectrochemical filter. Journal of Hazardous Materials, 2020, 389, 121840.	6.5	37
60	Rapid decontamination of tetracycline hydrolysis product using electrochemical CNT filter: Mechanism, impacting factors and pathways. Chemosphere, 2020, 244, 125525.	4.2	40
61	Comparison of pollutant source tracking approaches: Heavy metals deposited on urban road surfaces as a case study. Environmental Pollution, 2020, 266, 115253.	3.7	13
62	Toxicity and biotransformation of bisphenol S in freshwater green alga Chlorella vulgaris. Science of the Total Environment, 2020, 747, 141144.	3.9	22
63	Toxicity variability of urban road stormwater during storage processes in Shenzhen, China: Identification of primary toxicity contributors and implications for reuse safety. Science of the Total Environment, 2020, 745, 140964.	3.9	11
64	Selective chelating precipitation of palladium metal from electroplating wastewater using chitosan and its derivative. Adsorption Science and Technology, 2020, 38, 113-126.	1.5	17
65	C3N4 modified with single layer ZIF67 nanoparticles for efficient photocatalytic degradation of organic pollutants under visible light. Chinese Journal of Catalysis, 2020, 41, 1894-1905.	6.9	46
66	Synthesis of magnetic recoverable electron-rich TCTA@PVP based conjugated polymer for photocatalytic water remediation and disinfection. Separation and Purification Technology, 2020, 250, 116954.	3.9	29
67	Design of a p–n heterojunction in 0D/3D MoS ₂ /g-C ₃ N ₄ composite for boosting the efficient separation of photogenerated carriers with enhanced visible-light-driven H ₂ evolution. RSC Advances, 2020, 10, 19169-19177.	1.7	18
68	Engineering 3D electron and ion transport channels by constructing sandwiched holey quaternary metal oxide nanosheets for high-performance flexible energy storage. Science China Materials, 2020, 63, 1719-1730.	3.5	7
69	Visible light responsive photoactive polymer supported on carbonaceous biomass for photocatalytic water remediation. Journal of Cleaner Production, 2020, 269, 122286.	4.6	34
70	Nanocapsulation of horseradish peroxidase (HRP) enhances enzymatic performance in removing phenolic compounds. International Journal of Biological Macromolecules, 2020, 150, 814-822.	3.6	45
71	Quantitative source tracking of heavy metals contained in urban road deposited sediments. Journal of Hazardous Materials, 2020, 393, 122362.	6.5	59
72	A Bifunctional Electroactive Ti4O7-Based Membrane System for Highly Efficient Ammonia Decontamination. Catalysts, 2020, 10, 383.	1.6	5

#	Article	IF	CITATIONS
73	CuO NPs incorporated into electron-rich TCTA@PVP photoactive polymer for the photocatalytic oxidation of dyes and bacteria inactivation. Journal of Water Process Engineering, 2020, 36, 101238.	2.6	11
74	Electrochemical sensor based on ZIF-8@dimethylglyoxime and \hat{l}^2 -cyclodextrin modified reduced graphene oxide for nickel (II) detection. Sensors and Actuators B: Chemical, 2020, 315, 128091.	4.0	32
75	Pb-Based Perovskite Solar Cells and the Underlying Pollution behind Clean Energy: Dynamic Leaching of Toxic Substances from Discarded Perovskite Solar Cells. Journal of Physical Chemistry Letters, 2020, 11, 2812-2817.	2.1	84
76	Broadband graphene-on-silicon modulator with orthogonal hybrid plasmonic waveguides. Nanophotonics, 2020, 9, 1529-1538.	2.9	19
77	Black phosphorus (BP)–graphene guided-wave surface plasmon resonance (GWSPR) biosensor. Nanophotonics, 2020, 9, 4265-4272.	2.9	18
78	Tuning the N-bonded cerium(<scp>iii</scp>) fraction/g-C ₃ N ₄ interface in hollow structures using an <i>in situ</i> reduction treatment for superior photochemical hydrogen evolution. Catalysis Science and Technology, 2019, 9, 5322-5332.	2.1	16
79	Continuous preparation of high performance flexible asymmetric supercapacitor with a very fast, low-cost, simple and scalable electrochemical co-deposition method. Journal of Power Sources, 2019, 437, 226827.	4.0	15
80	Preparation, Stabilization and Carbonization of a Novel Polyacrylonitrile-Based Carbon Fiber Precursor. Polymers, 2019, 11, 1150.	2.0	59
81	Sustainable self-floating lignocellulosic biomass-TiO2@Aerogel for outdoor solar photocatalytic Cr(VI) reduction. Separation and Purification Technology, 2019, 229, 115830.	3.9	36
82	Effects of dechlorination conditions on the developmental toxicity of a chlorinated saline primary sewage effluent: Excessive dechlorination is better than not enough. Science of the Total Environment, 2019, 692, 117-126.	3.9	27
83	Behaviour of metals in an urban river and the pollution of estuarine environment. Water Research, 2019, 164, 114911.	5.3	35
84	Microbial reduction of bromate: current status and prospects. Biodegradation, 2019, 30, 365-374.	1.5	8
85	Rethinking hydrocarbons build-up on urban roads: A perspective on volatilisation under global warming scenarios. Environmental Pollution, 2019, 252, 950-959.	3.7	3
86	Identification, Formation, and Predicted Toxicity of Halogenated DBPs Derived from Tannic Acid and Its Biodegradation Products. Environmental Science & Technology, 2019, 53, 13019-13030.	4.6	22
87	Tea Residue Boosts Dye Decolorization and Induces the Evolution of Bacterial Community. Water, Air, and Soil Pollution, 2019, 230, 1.	1.1	3
88	Boosting Cr(VI) detoxification and sequestration efficiency with carbon nanotube electrochemical filter functionalized with nanoscale polyaniline: Performance and mechanism. Science of the Total Environment, 2019, 695, 133926.	3.9	32
89	Factors influencing volatile hydrocarbon pollution in urban areas. Emerging Contaminants, 2019, 5, 288-296.	2.2	2
90	Enhancement of Ni/NiO/graphitized carbon and β-Cyclodextrin/reduced graphene oxide for the electrochemical detection of norfloxacin in water sample. Journal of Electroanalytical Chemistry, 2019, 851, 113407.	1.9	18

#	Article	IF	CITATIONS
91	Enhanced photoelectrocatalytic breakdown of Cu-cyanide complexes and copper recovery using photoelectrogenerated free chlorine. Electrochemistry Communications, 2019, 100, 34-38.	2.3	11
92	Enhanced photoelectrocatalytic degradation of bisphenol A and simultaneous production of hydrogen peroxide in saline wastewater treatment. Chemosphere, 2019, 222, 141-148.	4.2	27
93	Durability and performance of loofah sponge as carrier for wastewater treatment with high ammonium. Water Environment Research, 2019, 91, 581-587.	1.3	13
94	Comparative toxicity of organic mixture attached to road deposited sediments: Inadequacy of conventionally using individual pollutants to assess comprehensive hazard effects. Ecotoxicology and Environmental Safety, 2019, 180, 357-365.	2.9	4
95	Unravelling the mechanistic role of Ti O C bonding bridge at titania/lignocellulosic biomass interface for Cr(VI) photoreduction under visible light. Journal of Colloid and Interface Science, 2019, 553, 409-417.	5.0	76
96	Toxic effects and metabolic fate of carbamazepine in diatom Navicula sp. as influenced by humic acid and nitrogen species. Journal of Hazardous Materials, 2019, 378, 120763.	6.5	16
97	Microbial characterization of heavy metal resistant bacterial strains isolated from an electroplating wastewater treatment plant. Ecotoxicology and Environmental Safety, 2019, 181, 472-480.	2.9	49
98	Amphiphilic Graphene Aerogel with High Oil and Water Adsorption Capacity and High Contact Area for Interface Reaction. ACS Applied Materials & Interfaces, 2019, 11, 22794-22800.	4.0	42
99	Unveiling the activating mechanism of tea residue for boosting the biological decolorization performance of refractory dye. Chemosphere, 2019, 233, 110-119.	4.2	12
100	Sustainable and easy recoverable magnetic TiO2-Lignocellulosic Biomass@Fe3O4 for solar photocatalytic water remediation. Journal of Cleaner Production, 2019, 233, 841-847.	4.6	68
101	Leaf-like 2D nanosheet as efficient oxygen reduction reaction catalyst for Zn-air battery. Journal of Power Sources, 2019, 434, 226717.	4.0	30
102	Application of (LC/)MS/MS precursor ion scan for evaluating the occurrence, formation and control of polar halogenated DBPs in disinfected waters: A review. Water Research, 2019, 158, 322-337.	5.3	157
103	Nutrients and metals interactions between water and sediment phases: An urban river case study. Environmental Pollution, 2019, 251, 354-362.	3.7	52
104	Fabrication of MnO2â€ʿcarbonized cotton yarn derived hierarchical porous active carbon flexible supercapacitor electrodes for potential applications in cable-type devices. Applied Surface Science, 2019, 487, 180-188.	3.1	33
105	Recent advances on photocatalytic fuel cell for environmental applications—The marriage of photocatalysis and fuel cells. Science of the Total Environment, 2019, 668, 966-978.	3.9	144
106	Morphology-controlled synthesis of hollow Si/C composites based on KI-assisted magnesiothermic reduction for high performance Li-ion batteries. Applied Surface Science, 2019, 481, 933-939.	3.1	30
107	Decomplexation removal of Ni(II)-citrate complexes through heterogeneous Fenton-like process using novel CuO-CeO2-CoOx composite nanocatalyst. Journal of Hazardous Materials, 2019, 374, 167-176.	6.5	46
108	Simultaneous achievement of refractory pollutant removal and energy production in the saline wastewater treatment. Chemical Engineering Journal, 2019, 369, 845-853.	6.6	11

#	Article	IF	CITATIONS
109	Surface modification of graphite by ion implantation for promoting the electrochemical property in Li-ion batteries. Applied Surface Science, 2019, 484, 726-731.	3.1	21
110	Carbonaceous biomass-titania composites with Ti O C bonding bridge for efficient photocatalytic reduction of Cr(VI) under narrow visible light. Chemical Engineering Journal, 2019, 366, 172-180.	6.6	113
111	Robust Linear Programming and Its Application to Water and Environmental Decision-Making under Uncertainty. Sustainability, 2019, 11, 33.	1.6	27
112	Recovery of Ni(II) from real electroplating wastewater using fixed-bed resin adsorption and subsequent electrodeposition. Frontiers of Environmental Science and Engineering, 2019, 13, 1.	3.3	32
113	Simultaneous Cr(VI) removal and bisphenol A degradation in a solar-driven photocatalytic fuel cell with dopamine modified carbon felt cathode. Applied Surface Science, 2019, 471, 912-920.	3.1	18
114	Comprehensive Insights into the Interactions of Two Emerging Bromophenolic DBPs with Human Serum Albumin by Multispectroscopy and Molecular Docking. ACS Omega, 2019, 4, 563-572.	1.6	40
115	Gaseous bubble-assisted in-situ construction of worm-like porous g-C3N4 with superior visible light photocatalytic performance. Applied Catalysis A: General, 2019, 573, 13-21.	2.2	24
116	Performance and microbial protein expression during anaerobic treatment of alkali-decrement wastewater using a strengthened circulation anaerobic reactor. Bioresource Technology, 2019, 273, 40-48.	4.8	3
117	Effective degradation of refractory nitrobenzene in water by the natural 4-hydroxycoumarin under solar illumination. Chemosphere, 2019, 215, 199-205.	4.2	10
118	Enhancement of municipal sludge dewaterability by electrochemical pretreatment. Journal of Environmental Sciences, 2019, 75, 98-104.	3.2	22
119	Hierarchically porous carbon derived from waste acrylic fibers for super-high capacity lithium ion battery anodes. Chemical Engineering Journal, 2018, 346, 143-150.	6.6	32
120	A simple approach to fabricate of Ni-NiCo2O4@ZnCo2O4 yolk-shell nano-tetrahedron composite as high-performance anode material for lithium-ion batteries. Chemical Engineering Journal, 2018, 341, 601-609.	6.6	30
121	Coupling Mo2C@C core-shell nanocrystals on 3D graphene hybrid aerogel for high-performance lithium ion battery. Applied Surface Science, 2018, 441, 69-76.	3.1	25
122	Correlating microbial community structure with operational conditions in biological aerated filter reactor for efficient nitrogen removal of municipal wastewater. Bioresource Technology, 2018, 250, 374-381.	4.8	31
123	Causes and mechanisms on the toxicity of layered double hydroxide (LDH) to green algae Scenedesmus quadricauda. Science of the Total Environment, 2018, 635, 1004-1011.	3.9	30
124	Ultrahighâ€ S trength Ultrahigh Molecular Weight Polyethylene (UHMWPE)â€Based Fiber Electrode for High Performance Flexible Supercapacitors. Advanced Functional Materials, 2018, 28, 1707351.	7.8	44
125	MOF-derived nitrogen doped carbon modified g-C3N4 heterostructure composite with enhanced photocatalytic activity for bisphenol A degradation with peroxymonosulfate under visible light irradiation. Applied Catalysis B: Environmental, 2018, 233, 35-45.	10.8	331
126	NiS2@CoS2 nanocrystals encapsulated in N-doped carbon nanocubes for high performance lithium/sodium ion batteries. Energy Storage Materials, 2018, 11, 67-74.	9.5	346

#	Article	IF	CITATIONS
127	Synergistic effect of ball-milled Al micro-scale particles with vitamin B12 on the degradation of 2,2′,4,4′-tetrabromodiphenyl ether in liquid system. Chemical Engineering Journal, 2018, 333, 613-620.	6.6	20
128	Ultrahigh level nitrogen/sulfur co-doped carbon as high performance anode materials for lithium-ion batteries. Carbon, 2018, 126, 85-92.	5.4	99
129	Biodegradation of triclosan in diatom Navicula sp.: Kinetics, transformation products, toxicity evaluation and the effects of pH and potassium permanganate. Journal of Hazardous Materials, 2018, 344, 200-209.	6.5	32
130	Anaerobic biodegradation and decolorization of a refractory acid dye by a forward osmosis membrane bioreactor. Environmental Science: Water Research and Technology, 2018, 4, 272-280.	1.2	27
131	Biouptake, toxicity and biotransformation of triclosan in diatom Cymbella sp. and the influence of humic acid. Environmental Pollution, 2018, 234, 231-242.	3.7	57
132	Effective degradation of carbamazepine using a novel electro-peroxone process involving simultaneous electrochemical generation of ozone and hydrogen peroxide. Electrochemistry Communications, 2018, 86, 26-29.	2.3	27
133	A recyclable self-assembled composite catalyst consisting of Fe ₃ O ₄ -rose bengal-layered double hydroxides for highly efficient visible light photocatalysis in water. Chemical Communications, 2018, 54, 13587-13590.	2.2	29
134	A g-C ₃ N ₄ /MIL-101(Fe) heterostructure composite for highly efficient BPA degradation with persulfate under visible light irradiation. Journal of Materials Chemistry A, 2018, 6, 23703-23711.	5.2	153
135	A Conductive and Highly Deformable Allâ€Pseudocapacitive Composite Paper as Supercapacitor Electrode with Improved Areal and Volumetric Capacitance. Small, 2018, 14, e1803786.	5.2	158
136	Sodium-Ion Batteries: SnS2 Nanosheets Coating on Nanohollow Cubic CoS2 /C for Ultralong Life and High Rate Capability Half/Full Sodium-Ion Batteries (Small 41/2018). Small, 2018, 14, 1870187.	5.2	2
137	Recent advances in anaerobic biological processes for textile printing and dyeing wastewater treatment: a mini-review. World Journal of Microbiology and Biotechnology, 2018, 34, 165.	1.7	85
138	Effective mineralization of anti-epilepsy drug carbamazepine in aqueous solution by simultaneously electro-generated H2O2/O3 process. Electrochimica Acta, 2018, 290, 203-210.	2.6	22
139	Organic Cotton Photocatalysis. ACS Sustainable Chemistry and Engineering, 2018, 6, 14759-14766.	3.2	27
140	SnS ₂ Nanosheets Coating on Nanohollow Cubic CoS ₂ /C for Ultralong Life and High Rate Capability Half/Full Sodiumâ€ion Batteries. Small, 2018, 14, e1802716.	5.2	93
141	Crystallization kinetics of Na ₂ CO ₃ in Bayer aluminate solutions during the evaporation process. CrystEngComm, 2018, 20, 3722-3727.	1.3	4
142	Performance evaluation of anaerobic baffled reactor (ABR) for treating alkali-decrement wastewater of polyester fabrics at incremental organic loading rates. Water Science and Technology, 2018, 77, 2445-2453.	1.2	19
143	Treatment of industrial dyeing wastewater with a pilot-scale strengthened circulation anaerobic reactor. Bioresource Technology, 2018, 264, 154-162.	4.8	63
144	Characterization of household food waste and strategies for its reduction: A Shenzhen City case study. Waste Management, 2018, 78, 426-433.	3.7	72

#	Article	IF	CITATIONS
145	Controllable synthesis of graphitic carbon nitride nanomaterials for solar energy conversion and environmental remediation: the road travelled and the way forward. Catalysis Science and Technology, 2018, 8, 4576-4599.	2.1	99
146	Persulfate enhanced photoelectrocatalytic degradation of cyanide using a CuFe2O4 modified graphite felt cathode. Chemical Engineering Journal, 2018, 347, 535-542.	6.6	44
147	Polydimethylsiloxane Sponge‣upported Nanometer Gold: Highly Efficient Recyclable Catalyst for Crossâ€Dehydrogenative Coupling in Water. ChemSusChem, 2018, 11, 3586-3590.	3.6	19
148	Biomass-derived nitrogen/oxygen co-doped hierarchical porous carbon with a large specific surface area for ultrafast and long-life sodium-ion batteries. Applied Surface Science, 2018, 462, 713-719.	3.1	41
149	Granulation process in an expanded granular sludge blanket (EGSB) reactor for domestic sewage treatment: Impact of extracellular polymeric substances compositions and evolution of microbial population. Bioresource Technology, 2018, 269, 153-161.	4.8	60
150	Degradation Characteristics of Color Index Direct Blue 15 Dye Using Iron-Carbon Micro-Electrolysis Coupled with H2O2. International Journal of Environmental Research and Public Health, 2018, 15, 1523.	1.2	24
151	Microgel-Enhanced Double Network Hydrogel Electrode with High Conductivity and Stability for Intrinsically Stretchable and Flexible All-Gel-State Supercapacitor. ACS Applied Materials & Interfaces, 2018, 10, 19323-19330.	4.0	62
152	N-doped foam flame retardant polystyrene derived porous carbon as an efficient scaffold for lithium-selenium battery with long-term cycling performance. Chemical Engineering Journal, 2018, 350, 411-418.	6.6	23
153	Enhanced primary sludge sonication by heat insulation to reclaim carbon source for biological phosphorous removal. Ultrasonics Sonochemistry, 2017, 34, 123-129.	3.8	6
154	Three-step effluent chlorination increases disinfection efficiency and reduces DBP formation and toxicity. Chemosphere, 2017, 168, 1302-1308.	4.2	98
155	Electrochemical mineralization of perfluorooctane sulfonate by novel F and Sb co-doped Ti/SnO 2 electrode containing Sn-Sb interlayer. Chemical Engineering Journal, 2017, 316, 296-304.	6.6	74
156	Organic sponge photocatalysis. Green Chemistry, 2017, 19, 2925-2930.	4.6	57
157	Toxicity, degradation and metabolic fate of ibuprofen on freshwater diatom Navicula sp Journal of Hazardous Materials, 2017, 330, 127-134.	6.5	163
158	Mn assisted electrochemical generation of two-dimensional Fe-Mn layered double hydroxides for efficient Sb(V) removal. Journal of Hazardous Materials, 2017, 336, 33-40.	6.5	42
159	Characterization of post-disaster environmental management for Hazardous Materials Incidents: Lessons learnt from the Tianjin warehouse explosion, China. Journal of Environmental Management, 2017, 199, 21-30.	3.8	34
160	H ₂ O ₂ Assisted Photoelectrocatalytic Oxidation of Ag-Cyanide Complexes at Metal-free g-C ₃ N ₄ Photoanode with Simultaneous Ag Recovery. ACS Sustainable Chemistry and Engineering, 2017, 5, 5001-5007.	3.2	39
161	Biodegradation of naproxen by freshwater algae Cymbella sp. and Scenedesmus quadricauda and the comparative toxicity. Bioresource Technology, 2017, 238, 164-173.	4.8	133
162	Bifunctional organic sponge photocatalyst for efficient cross-dehydrogenative coupling of tertiary amines to ketones. Chemical Communications, 2017, 53, 12536-12539.	2.2	44

#	Article	IF	CITATIONS
163	Bacterial and archaeal community distribution and stabilization of anaerobic sludge in a strengthen circulation anaerobic (SCA) reactor for municipal wastewater treatment. Bioresource Technology, 2017, 244, 750-758.	4.8	31
164	Directed Aromatic C–H Activation/Acetoxylation Catalyzed by Pd Nanoparticles Supported on Graphene Oxide. Organic Letters, 2017, 19, 6470-6473.	2.4	26
165	NiFe2O4 porous nanorods/graphene composites as high-performance anode materials for lithium-ion batteries. Electrochimica Acta, 2017, 248, 292-298.	2.6	34
166	DOSIMETRIC EVALUATION OF LASER-DRIVEN X-RAY AND NEUTRON SOURCES UTILIZING XG-III PS LASER WITH PEAK POWER OF 300 TERAWATT. Radiation Protection Dosimetry, 2017, 177, 302-309.	0.4	3
167	Synergistic effect of ferrous ion and copper oxide on the oxidative degradation of aqueous acetaminophen at acid conditions: A mechanism investigation. Chemical Engineering Journal, 2017, 326, 612-619.	6.6	23
168	Performance and microbial community structures of hydrolysis acidification process treating azo and anthraquinone dyes in different stages. Environmental Science and Pollution Research, 2017, 24, 252-263.	2.7	28
169	Copper–catalyzed activation of molecular oxygen for oxidative destruction of acetaminophen: The mechanism and superoxide-mediated cycling of copper species. Chemosphere, 2017, 166, 89-95.	4.2	80
170	Electrochemical Oxidation of Environmentally Persistent Perfluorooctane Sulfonate by a Novel Lead Dioxide Anode. Electrochimica Acta, 2016, 213, 358-367.	2.6	58
171	Biofouling behavior and performance of forward osmosis membranes with bioinspired surface modification in osmotic membrane bioreactor. Bioresource Technology, 2016, 211, 751-758.	4.8	40
172	Highly efficient removal of perfluorooctanoic acid from aqueous solution by H 2 O 2 -enhanced electrocoagulation-electroflotation technique. Emerging Contaminants, 2016, 2, 49-55.	2.2	31
173	Characterization of brominated flame retardants in construction and demolition waste components: HBCD and PBDEs. Science of the Total Environment, 2016, 572, 77-85.	3.9	43
174	Carbon-coated LiFePO4synthesized by a simple solvothermal method. CrystEngComm, 2016, 18, 7537-7543.	1.3	12
175	A mechanically synthesized SiO ₂ –Fe metal matrix composite for effective dechlorination of aqueous 2-chlorophenol: the optimum of the preparation conditions. RSC Advances, 2016, 6, 76867-76873.	1.7	11
176	Impact of Biological Treatment Techniques on Perfluoroalkyl Acids Emissions in Municipal Sewage. Water, Air, and Soil Pollution, 2016, 227, 1.	1.1	6
177	Influence of Soil Factors on the Stereoselective Fate of a Novel Chiral Insecticide, Paichongding, in Flooded Paddy Soils. Journal of Agricultural and Food Chemistry, 2016, 64, 8109-8117.	2.4	9
178	Efficient removal of perfluoroalkyl acids (PFAAs) from aqueous solution by electrocoagulation using iron electrode. Chemical Engineering Journal, 2016, 303, 384-390.	6.6	42
179	Enhanced phosphorus recovery and biofilm microbial community changes in an alternating anaerobic/aerobic biofilter. Chemosphere, 2016, 144, 1797-1806.	4.2	30
180	Novel iron metal matrix composite reinforced by quartz sand for the effective dechlorination of aqueous 2-chlorophenol. Chemosphere, 2016, 146, 308-314.	4.2	18

#	Article	IF	CITATIONS
181	The pathogenesis of rheumatoid arthritis is associated with milk or egg allergy. North American Journal of Medical Sciences, 2016, 8, 40.	1.7	13
182	Spatial distribution and partition of perfluoroalkyl acids (PFAAs) in rivers of the Pearl River Delta, southern China. Science of the Total Environment, 2015, 524-525, 1-7.	3.9	64
183	Highly efficient electrochemical degradation of perfluorooctanoic acid (PFOA) by F-doped Ti/SnO2 electrode. Journal of Hazardous Materials, 2015, 299, 417-424.	6.5	83
184	Perfluorinated compounds (PFCs) in the atmosphere of Shenzhen, China: Spatial distribution, sources and health risk assessment. Chemosphere, 2015, 138, 511-518.	4.2	69
185	Promoting effect of EDTA on catalytic activity of highly stable Al–Ni bimetal alloy for dechlorination of 2-chlorophenol. Chemical Engineering Journal, 2014, 250, 222-229.	6.6	33
186	Electrochemical oxidation of 1H,1H,2H,2H-perfluorooctane sulfonic acid (6:2 FTS) on DSA electrode: Operating parameters and mechanism. Journal of Environmental Sciences, 2014, 26, 1733-1739.	3.2	32
187	Reductive degradation of chlorinated organic pollutants-contaminated water by bimetallic Pd/Al nanoparticles: Effect of acidic condition and surfactants. Chemical Engineering Journal, 2013, 234, 346-353.	6.6	24
188	Shaddock peel as a novel low-cost adsorbent for removal of methylene blue from dye wastewater. Desalination and Water Treatment, 2012, 39, 70-75.	1.0	16
189	Anaerobic Baffled Reactor (ABR) for Alkali-minimization Dyeing-printing Wastewater Biodegradation. , 2012, , .		2
190	Degradation of perfluorinated compounds on a boron-doped diamond electrode. Electrochimica Acta, 2012, 77, 17-22.	2.6	172
191	Efficient Electrochemical Oxidation of Perfluorooctanoate Using a Ti/SnO ₂ -Sb-Bi Anode. Environmental Science & Technology, 2011, 45, 2973-2979.	4.6	305
192	Bimetallic Pd/Al particles for highly efficient hydrodechlorination of 2-chlorobiphenyl in acidic aqueous solution. Journal of Hazardous Materials, 2011, 189, 76-83.	6.5	57
193	Catalytic Hydrodechlorination of 4-Chlorophenol in an Aqueous Solution with Pd/Ni Catalyst and Formic Acid. Industrial & Engineering Chemistry Research, 2010, 49, 4561-4565.	1.8	50
194	Notice of Retraction: Influence of Organizational Boundary on Psychological Empowerment in Multi-organization Network. , 2009, , .		0
195	Readout system of the multi-level read-only disc using signal waveform modulation. , 2009, , .		0
196	The Third Contribution of Knowledge Management to Business Process. , 2007, , .		1
197	Electrocatalytic hydrodechlorination of 4-chlorobiphenyl in aqueous solution using palladized nickel foam cathode. Chemosphere, 2007, 67, 1361-1367.	4.2	66
198	Electrocatalytic Hydrodechlorination of 2,4,5-Trichlorobiphenyl on a Palladium-Modified Nickel Foam Cathode. Environmental Science & Technology, 2007, 41, 7503-7508.	4.6	109